International Journal of Sustainable Energy Planning and Management Vol. 06 2016 17-30

International Journal of
Sustainable Energy Planning and Management

Spatial Modelling of Solar Energy Potential in Kenya

Francis Oloo[1*], Luke Olang[2] and Josef Strobl[1]

[1]*Interfaculty Department of Geoinformatics, University of Salzburg, Austria*
[2]*Biosystems and Environmental Engineering, Technical University of Kenya, Nairobi, Kenya*

ABSTRACT

Solar energy is one of the readily available renewable energy resources in the developing countries within the tropical region. Kenya is one of the countries which receive an average of approximately 6.5 sunshine hours in a single day throughout the year. However, there is slow adoption of solar energy resources in the country due to limited information on the spatial variability solar energy potential. This study aims at assessing the potential of photovoltaic solar energy in Kenya. The factors that influence incident solar radiation which were considered in this task included atmospheric transmissivity and topography. The influence of atmospheric transmissivity was factored in by modeling monthly transmissivity factors from a combination of cloud cover, diffuse ratios and the effect of altitude. The contribution of topography was included by applying hemispherical view shed analysis to determine the amount of incident global radiation on the surface based on the orientation of the terrain. GIS concepts were used to integrate the spatial datasets from different themes. The results showed that, about 70% of the land area in Kenya has the potential of receiving approximately 5 kWh/m^2/day throughout the year. In outline, this work successfully assessed the spatio-temporal variability in the characteristics of solar energy potential in Kenya and can be used as a basis for policy support in the country.

Keywords:

Spatial modeling;
Solar energy;
Renewable energy;
GIS;
Kenya;
URL:
dx.doi.org/10.5278/ijsepm.2015.6.3

1. Introduction

Accessibility to reliable energy sources is critical to the development and well-being of every nation [1]. According to the Global Status Report on Renewable Energy 2012 [2], only 51% of Kenyans living in the urban areas have access to electricity while only 4% of those living in the rural areas have access to electricity. Over the years, the primary electric energy supply in Kenya has been through traditional electricity generation sources such as hydro-electric power, thermal oil and geothermal power. The challenges associated with climate change have made reliance on hydro-electric power unpredictable. Additionally, increasing population growth rate continues to complicate energy supply and demand matrix in the country. Despite, these challenges, the geographic position of Kenya within the tropics and precisely on the equatorial region provides an opportunity for the country to tap from the readily available solar energy resources. Kenya is in fact, one of the countries in Africa where solar energy has been exploited albeit only marginally since 1970s [3]. The amount of incoming solar radiation incident on the surface of the earth directly from the sun is referred to as direct solar radiation while the amount of solar radiation that hits the earth surface after it has been scattered or reflected by objects within the atmosphere is referred to as diffuse solar radiation. The summation of direct and diffuse solar radiation is known as global solar radiation. The actual amount of solar radiation incident on a unit

* Corresponding author email: oloofrank@gmail.com

surface over a period of time is referred to as solar insolation [4].

Even though the amount of solar insolation incident on the earth surface can be measured, the spatial distribution of the measurement instruments and fine temporal resolution of the measured data cannot be obtained for every place and at every instance on the earth's surface [5], as a result the use of solar radiation models has been critical for many engineering and economic decisions. While some studies have used the measured meteorological data to estimate solar radiation at unmeasured locations, for instance [6] used measured meteorological data to analyse the relationship between daily global radiation and other meteorological and geographical factors. Other studies have used concepts and data from remote sensing to estimate solar radiation [7] and [8].

Furthermore, some studies have used a combination of satellite generated data and direct measurements to map the potential of solar energy. For instance, [9] mapped solar energy potential in Kanartaka, India from meteorological data. Similarly, [10] used satellite derived insolation data to map the solar energy hotspots in India. Satellite imagery has also been used for siting and for evaluating the performance of both thermal and photovoltaic solar radiation applications [11]. Apart from the varying data sources and models that have been used to assess solar energy potential, different methods have also been employed. [12] used a non-linear meteorological radiation model to assess global radiation characteristics in Rwanda while [13] modelled solar energy potential in Africa using artificial neural networks.

Most of the common spatial based models for evaluating the amount of incident solar radiation on the surface of the earth are based on the concepts of hemispherical photogrammetry [14]. The models use the proportion of unobstructed sky and the incident angle of radiation which is obtained from the sun's zenith angle to compute the amount of incident solar radiation at a particular location. Specifically, the concept is implemented in steps as follows. First, the angular distribution of sky obstruction is specified in hemispherical coordinates system and projected on a plane. Secondly, the sky is divided into discrete number of sectors based on the zenith angle and azimuth angle. The angular area of proportion of unobstructed sky in each sector is then computed. Thirdly, the proportion of each sky sector is multiplied by the irradiance corresponding to the entire sky sectors and also by a factor of cosine weighting for the angle of incidence between the sky sector and the earth surface. Finally, the calculated irradiance for all the sectors are combined to come up with the total incident solar radiation for the point of interest [15].[16] used solar radiation analyst tool within ArcGIS 10.2 to integrate meteorological data and digital surface models to estimate solar irradiation at a territorial level. Apart from the solar radiation analysis models that have been integrated in proprietary GIS software, [17] implemented the r.sun package within open source GIS package GRASS and successfully estimated insolation and photovoltaic yield in a case study in Canada.

1.1. Renewable energy situation in Kenya

Kenya has traditionally relied on hydro-power, thermal oil and geothermal energy as the main sources of electricity for the country. However, in 2004, the government introduced Sessional Paper no. 4 of 2004 in the energy sector whose aim was to diversify sources of energy and promote the development of renewable energy technology in the country [18]. Additionally, the paper looked at ways of promoting rural electrification to increase access to electricity throughout the country. The Energy Act No. 12 of December 2006 established the Energy Regulation Commission (ERC) as the body mandated to offer regulatory stewardship on electricity, petroleum and renewable energy sub-sectors in Kenya. The legislation aimed at promoting the development of renewable energy technologies and international cooperation on programs related to renewable energy. Additionally, the Act was intended to facilitate mainstreaming the utilization of renewable energy resources in electricity generation and in transportation. To facilitate resource mobilization for investment in renewable energy generation and to encourage the participation of private sector players in the process, Feed - In Tariffs (FiTs) Policy on wind, biomass, small-hydro, geothermal, biogas and solar resource generated electricity was introduced in 2010 [19]. However, [20] noted that whereas Kenya has promoted the use of large-scale renewable energy to fulfill the national power demand particular through the Feed-in Tariff policy, only marginal attention has been given to small-scale renewable energy resources thus limiting the benefits gained by the rural areas where the resources are largely found.

An assessment of the solar energy market in Kenya indicated that the market is segmented into three tiers. Specifically there are solar house systems and small-scale commercial applications systems which make up of about three-quarters of the installed capacity, secondly there are systems that provide off-grid electricity to schools, health centres, churches, missions and other social institutions in rural areas and finally there are solar powered base stations for mobile communication networks and tourism networks [3]. Increased income among rural residents especially in coffee and tea rich regions in Kenya has been a motivation for farmers in such areas to acquire solar PV systems [21]. Consequently, the improved solar electrification in rural areas has resulted to increased television use, the expansion of markets and other processes that lead to rural to urban communication like the proliferation of mobile phone technology [22]. [1] also noted that technology transfer where different government institutions and non-governmental organizations have been involved in training the rural residents on the benefits of adopting renewable energy sources as opposed to the traditional sources has also contributed greatly to the accessibility of solar PV systems in rural Kenya. According to the 2009 population census, 4% of households in Kenya were using solar energy as the main source of lighting.

In Kenya, various attempts have been made to assess the potential of solar energy generation. [23] used geostationary satellite data to model Global Horizontal Irradiation (GHI) and Direct Normal Irradiation (DHI) at 10km spatial resolution for the years 2000-2002. Their results were however not compared to ground measurements for validation. [24] analysed 8 year data in nine regions/sites in Kenya and observed that the country has an annual mean radiation of 6.98 kWh/m^2. However, in an assessment of renewable energy resource potential and status of exploitation in Kenya, [25] concluded that the country has an annual average potential of 5 kWh/m^2/day and that Kenya has the world's highest household solar ownership rate. In spite of the obvious benefits of renewable energy resources and the apparent solar energy potential in Kenya, the prohibitive costs of initiating commercially viable photovoltaic solar energy generating plants and lack of accurate information on potential opportunities and markets have been identified as the main hindrances to exploitation of solar energy in Kenya [26]. This study therefore aims at using GIS methods to model high resolution solar energy potential surfaces in Kenya. In appreciation of the fact that different factors have an influence on solar energy potential, GIS methods and tools are used to model and integrate different themes in order to generate potential solar radiation surfaces at 100m resolution spatial resolution and at a monthly epoch. Specifically, three themes were integrated in this work; these were cloud cover, atmospheric transmissivity and global radiation.

2. Methodology

2.1. Study area

This study was carried out in Kenya. Spatially, the country covers an area of approximately 580,300 km^2 and is located approximately between 5°S and 5° N in latitude and between 32°E and 42° E in longitudes. The country lies on the equatorial belt with approximately one half of the country in the southern hemisphere while the other half lies in the northern hemisphere. The full range of elevation in the country is between 0 and 5200 m above mean sea level. According to the 2009 Kenya National Population and Housing Census report, the country had a total population of 38,610,097 people. Figure 1 represents the area of study

2.2. Data and tools

Two main categories of data were used in this study; these were digital elevation model and climate data.

2.2.1. Elevation data

A 90m resolution digital elevation model was used in this study. The elevation model was obtained from CGIAR SRTM. Elevation is the main input for the ArcGIS 10.2 Solar Radiation analyst. Elevation data is the source of topographical characteristics of the study site including terrain shading, slope and aspect. These characteristics are important both for sighting of the high potential areas and for positioning of solar energy generation equipment. Figure 2 shows the map of elevation designed from the elevation model.

According to figure 2, it is evident that the coastal region towards the south eastern part of Kenya has the lowest elevation values. Mt. Kenya which located in the central part of the country is the highest point in the country standing at approximately 5000m above the mean sea level The other high altitude regions in the country are the Aberdare ranges, Cherenganyi ranges and Mt. Elgon on the western border with Uganda.

2.2.2. Typical Meteorological Year (TMY) data

In order to have common long term data in solar energy related studies, different methods have been developed

Figure 1: Map of the area of study, Kenya.

and applied to successfully generate typical meteorological data. The methods mainly rely on the available data within different years to simulate and predict the missing data as a way of filling in the gaps. Hourly solar radiation and TMY data that was used in this study were obtained from Solar and Wind Energy Resource Assessment (SWERA) datasets [27]. The data was available for 23 stations in Kenya between 1973 and 2002. The data from this source was used in the following ways; i) cloud cover data from all the 23 station was combined with cloud cover data from NASA-SSE to interpolate cloud cover surfaces for the area of study ii) Cloud cover surfaces which were interpolated purely from this data was used to validate the cloud cover surfaces which were interpolated from a combination of NASA-SSE and TMY data sources iii) Diffuse radiation and global radiation data from this source was used to estimate the monthly diffuse ratios which were then used as to parameterise the Solar Analyst model in ArcGIS 10 iv) estimated (measured) transmissivity factor and the global radiation data from this source was used to validate the modelled transmissivity factors and the solar radiation estimates. Table 1 shows the TMY stations whose data was available for this study.

2.2.3. Cloud cover data

Cloud cover data for this study was mainly sourced from NASA Surface Meteorology and Solar (NASA-SSE) radiation data. Cloud amounts data are part of over 200 satellite derived meteorology and solar radiation parameters [28] archived by NASA-SSE database. The data for a particular geographic location can be accessed by defining the spatial extents of the location (or the coordinates of the location in case only the data at a single location are needed). Once a region is defined, monthly data tables can be retrieved for a 90° by 90° extent at a time while annual data tables can be retrieved for a 10° by 10° region at a time. In this work, average cloud amount (%) data was retrieved for 03GMT, O6GMT, 09GMT, 12GMT and 15GMT time intervals. The choice of these particular data layers was based on the fact that Kenyan

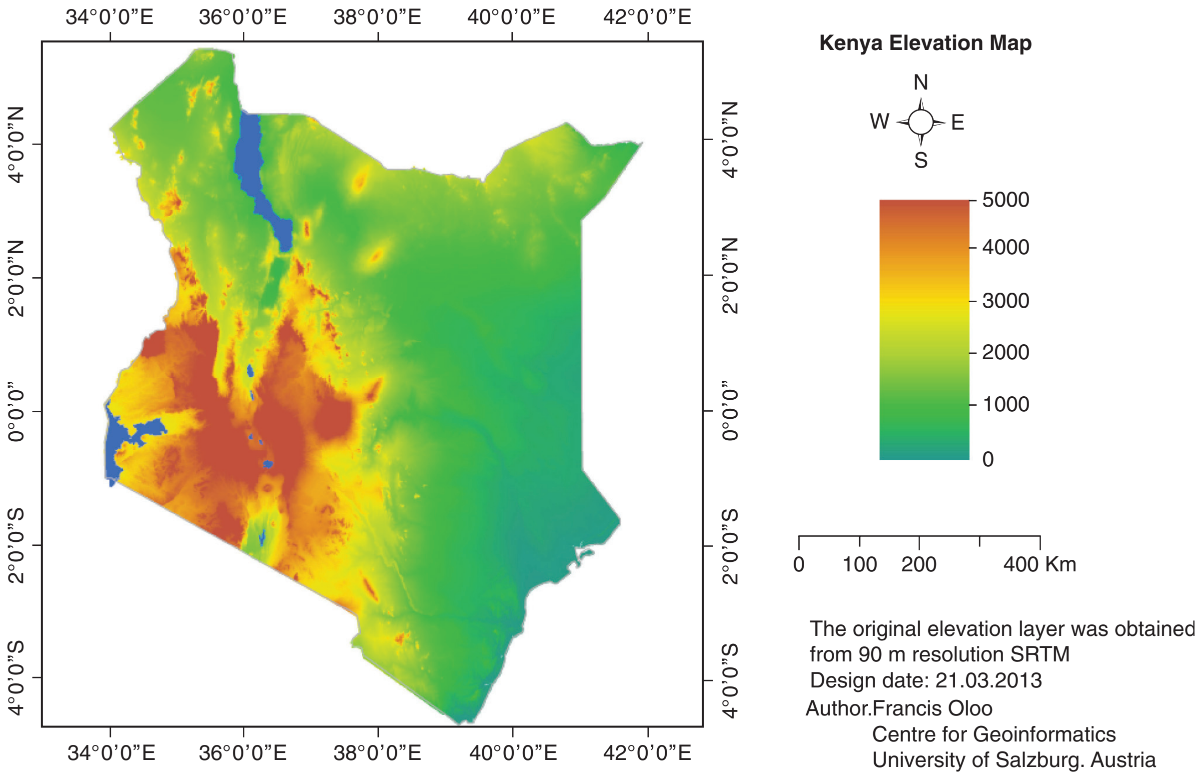

Figure 2: Map of elevation in Kenya.

Table 1: Names and locations of TMY stations considered in the study.

WMO Code	Station	Country	Latitude	Longitude	Elevation (m)
636120	Lodwar	Kenya	N 3 07	E 35 37	515
636190	Moyale	Kenya	N 3 32	E 39 03	1097
636240	Mandera	Kenya	N 3 56	E 41 52	231
636410	Marsabit	Kenya	N 2 18	E 37 54	1345
636610	Kitale	Kenya	N 1 01	E 35 00	1875
636860	Eldoret	Kenya	N 0 32	E 35 17	2133
636870	Kakamega	Kenya	N 0 17	E 34 47	1530
636950	Meru	Kenya	N 0 05	E 37 39	1554
637080	Kisumu	Kenya	S 0 06	E 34 45	1146
637090	Kisii	Kenya	S 0 40	E 34 47	1493
637140	Nakuru	Kenya	S 0 16	E 36 06	1901
637170	Nyeri	Kenya	S 0 30	E 36 58	1759
637200	Embu	Kenya	S 0 30	E 37 27	1493
637230	Garissa	Kenya	S 0 28	E 39 38	147
637370	Narok	Kenya	S 1 08	E 35 50	1890
637400	Nairobi (JKIA)	Kenya	S 1 19	E 36 55	1624
637410	Nairobi(Dagoretti)	Kenya	S 1 18	E 36 45	1798
637420	Nairobi(Wilson)	Kenya	S 1 19	E 36 49	1679
637660	Makindu	Kenya	S 2 17	E 37 50	1000
637720	Lamu	Kenya	S 2 16	E 40 50	6
637930	Voi	Kenya	S 3 24	E 38 34	579
637990	Malindi	Kenya	S 3 14	E 40 06	23
638200	Mombasa	Kenya	S 4 02	E 39 37	55

time is three hours ahead of the GMT time (+3.00 GMT) and therefore the selected datasets would represent 6am to 6pm in local Kenyan time at 3-hour intervals. The cloud data from NASA-SSE was combined with the cloud data from TMY stations as a way of calibrating the resulting cloud cover surfaces. Figure 3, shows the locations of NASA-SSE data points and the TMY station points.

A summarised workflow of the steps that were followed in this task is shown in figure 4.There were two main aspects of the methodology which were further divided into smaller steps. The first aspect involved the interpolation of representative monthly cloud cover surfaces. These were subsequently used to compute monthly transmissivity factors for the area of study. The second part on the other hand involved modelling representative monthly global radiation layers from the digital elevation model. Finally, the transmissivity factors were multiplied with the global radiation layers and combined with sunshine hours to result in the respective monthly average solar radiation potential surfaces.

2.3. Data processing

The average human settlement line around Mt. Kenya which is the highest mountain in Kenya is located approximately 3000m above mean sea level. Areas characterised by altitude values greater than 3000m above the mean sea level were thus excluded from the analysis. The original three-hour cloud cover data tables from NASA-SSE database was organized by rearranging the data fields so that, after the latitude and longitude columns, the monthly data appeared sequentially from January to December. This arrangement was important for the logical execution of the python script that was used to iteratively interpolate monthly cloud cover surfaces. Measured monthly cloud cover values from 23TMY stations were then added to the NASA-SSE cloud cover data tables. The intention of this was to use the measured values to calibrate the interpolated monthly cloud cover surfaces. The tabular data was georeferenced and converted to feature classes.

Inverse Distance Weighting (IDW) method of spatial interpolation was used to create monthly cloud cover surfaces. IDW method is a local and an exact

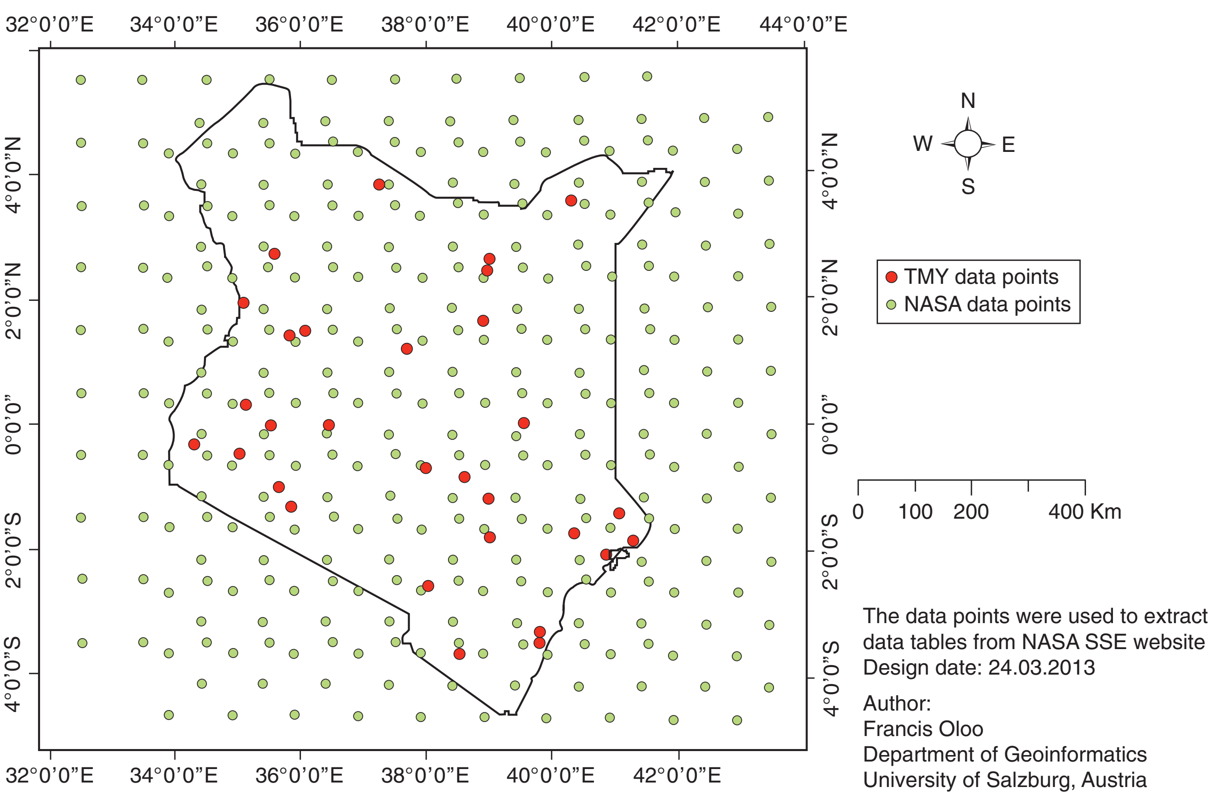

Figure 3: Map of NASA cloud cover data points and TMY station points.

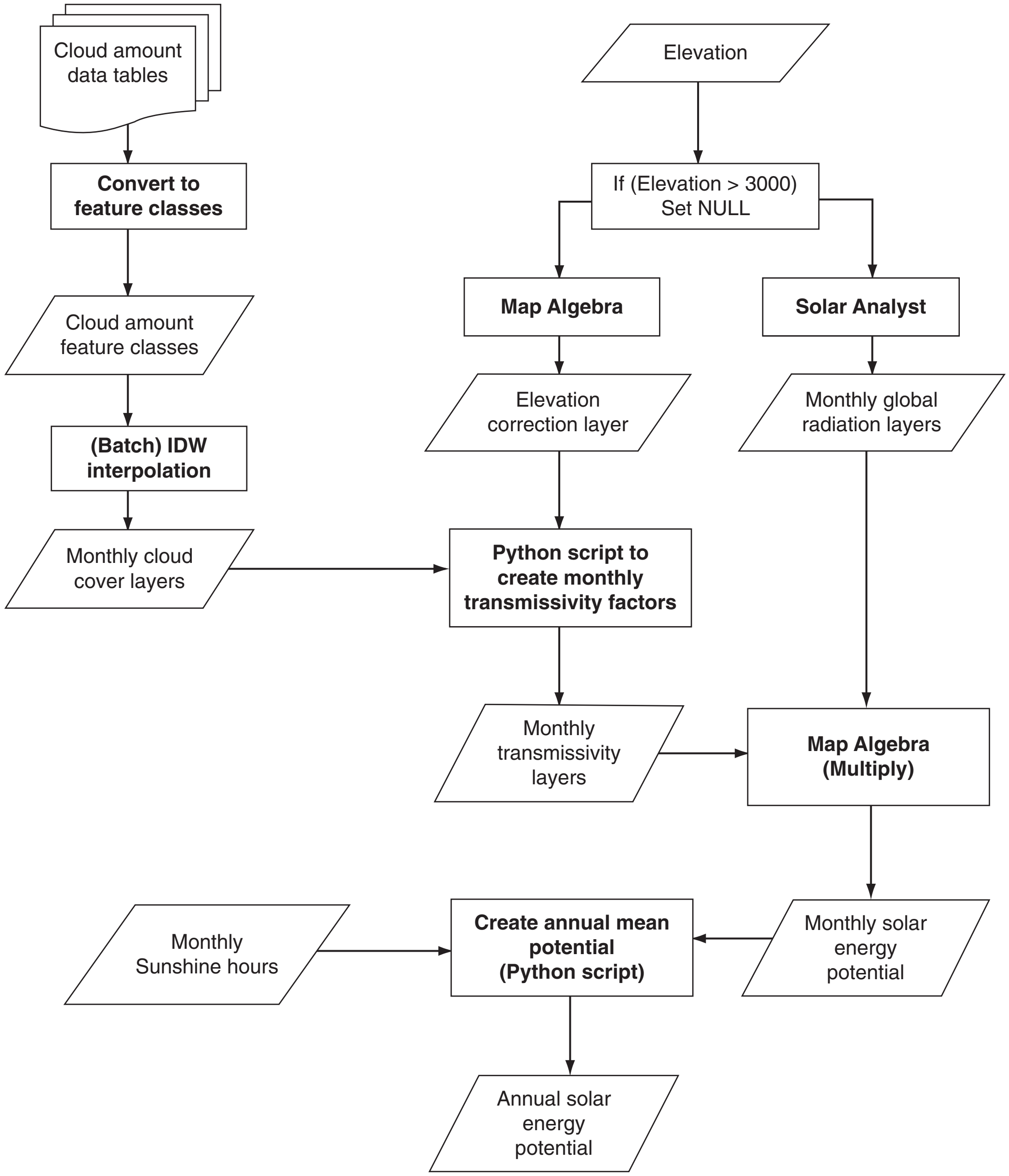

Figure 4: Summarised workflow for modelling solar energy potential.

interpolation method and was preferred as it ensures that interpolated values are as close as possible to the observed values and also restricts the interpolated values to the range of the observed data. The interpolation process was iteratively executed using a python script within ArcGIS 10.2.

The interpolated monthly cloud cover layers were then used to estimate monthly transmissivity surfaces. Transmissivity factor refers to the proportion of the incident radiation at the top of the atmosphere that successfully penetrates through the atmosphere to hit the ground surface. Transmissivity factor can be computed as the quotient of the global solar radiation incident on a horizontal surface and the extra-terrestrial horizontal radiation [7] and [29]. Additionally, since physiographic characteristics of terrain including elevation, slope, aspect and topographic convergence have been found to have in an influence on meteorological elements including solar insolation [30], an elevation factor equivalent to the product of $2.2 \times 10 - 5$ [31] and elevation at a particular station should be added to the transmission factor to increase transmittance with altitude [32]. We used a simplified formula introduced by [7] to estimate monthly transmissivity factors from the monthly cloud cover surfaces. In the formula, the relationship between transmissivity factors for an overcast sky k_b, transmissivity factor for a clear sky k_c and the cloud cover index n^t can be used to estimate a representative transmission factor k^t at a particular location.

$$k^t = n^t\, k_b + (1 - n^t)\, k_c$$

We calculated representative transmission factors for clear sky k_c and the transmission for an overcast sky k_b as ratios of daily incident global radiation and daily extra-terrestrial radiation from each of the 23 stations. An average of the calculated maximum transmissivity factor from the 23 stations was assigned to k_c, specifically, the value was 0.83. On the other hand the transmissivity factor for an overcast sky was set at 0.12. This value was calculated from as an average of the minimum transmissivity factors at the 23 TMY stations. Monthly cloud cover surfaces were used to represent the cloud cover index n_t.

2.4. Modelling solar radiation potential

The second aspect of the solar energy model involved estimating representative monthly global radiation layers from the elevation surface. Solar Radiation Analyst tool in ArcGIS 10.2 was used to estimate global solar radiation surfaces. The Solar Radiation Analyst tool uses the relationship between elevation, visible sky size, transmission factor, diffusion ratio and sky obstruction caused by features in the vicinity of the location of interest to compute the amount of solar insolation incident on that particular location [33]. Specifically, [34] identified that topography has two important influences on the amount of insolation at a particular location. Firstly, the orientation of the surface determines the angle of incidence of solar radiation on the surface. Secondly, the features in the vicinity of the location of interest determine the amount of insolation that can be incident on that location. Apart from the elevation model, the other inputs in the Solar Radiation Analysis tool include theoretical and empirical values of transmissivity factor and diffuse ratio among others [33] [14].Monthly diffuse ratios were computed from the station data.

In this work, we configured the Solar Radiation Analyst tool within ArcGIS 10.2 to estimate the solar radiation for every 10 days within a month, for each day in the analysis; the model was configured to estimate a radiation surface for every quarter of an hour (0.25 hours). The overall global radiation surface for that specific day was computed as a summation of the quarter-hour surfaces. The 10-day global radiation surfaces were then used to compute monthly average radiation surfaces. The final step in the analysis involved multiplying the estimated monthly global radiation surfaces by monthly transmissivity factors to obtain representative potential monthly solar energy surfaces for the area of study.

3. Results

We obtained three main sets of results from this study, these were, interpolated monthly cloud cover surfaces, monthly transmissivity factor surfaces and monthly potential solar radiation surfaces. In this paper, we only present and analyse the results of monthly transmissivity factors and the potential monthly radiation solar radiation surfaces.

3.1. Estimated monthly transmissivity factors

Figure 5 shows the maps of estimated transmissivity factors for each month in Kenya. In the context of this work, transmissivity was perceived as the proportion of incident radiation at the top of the atmosphere that successfully penetrates through the clouds and was computed from cloud cover, diffusion ratio and correction for the effect of elevation.

From the maps of monthly transmissivity factors represented in figure 5, we noted that the highest values of transmissivity factors were estimated in the months of February, September and January respectively. Specifically the average transmissivity in February, September and January was 0.54, 0.53 and 0.54. On the other hand, the lowest value of average transmissivity was estimated in April at 0.41 implying that only 40% of incident radiation above the atmosphere would penetrate through the atmosphere in the month of April. It was also observed that the northern part of the country towards the eastern side of Lake Turkana consistently recorded higher values of transmissivity factor. Additionally, with the exception of the month of February, the south coastal part of the country was consistently characterized by transmissivity factors of approximately 0.4–0.5 in all the other months.

3.2. Validation of estimated transmissivity factors against measured transmissivity factors

Monthly transmissivity factors that were calculated as quotients of global horizontal radiation and extraterrestrial horizontal radiation were compared to the estimated

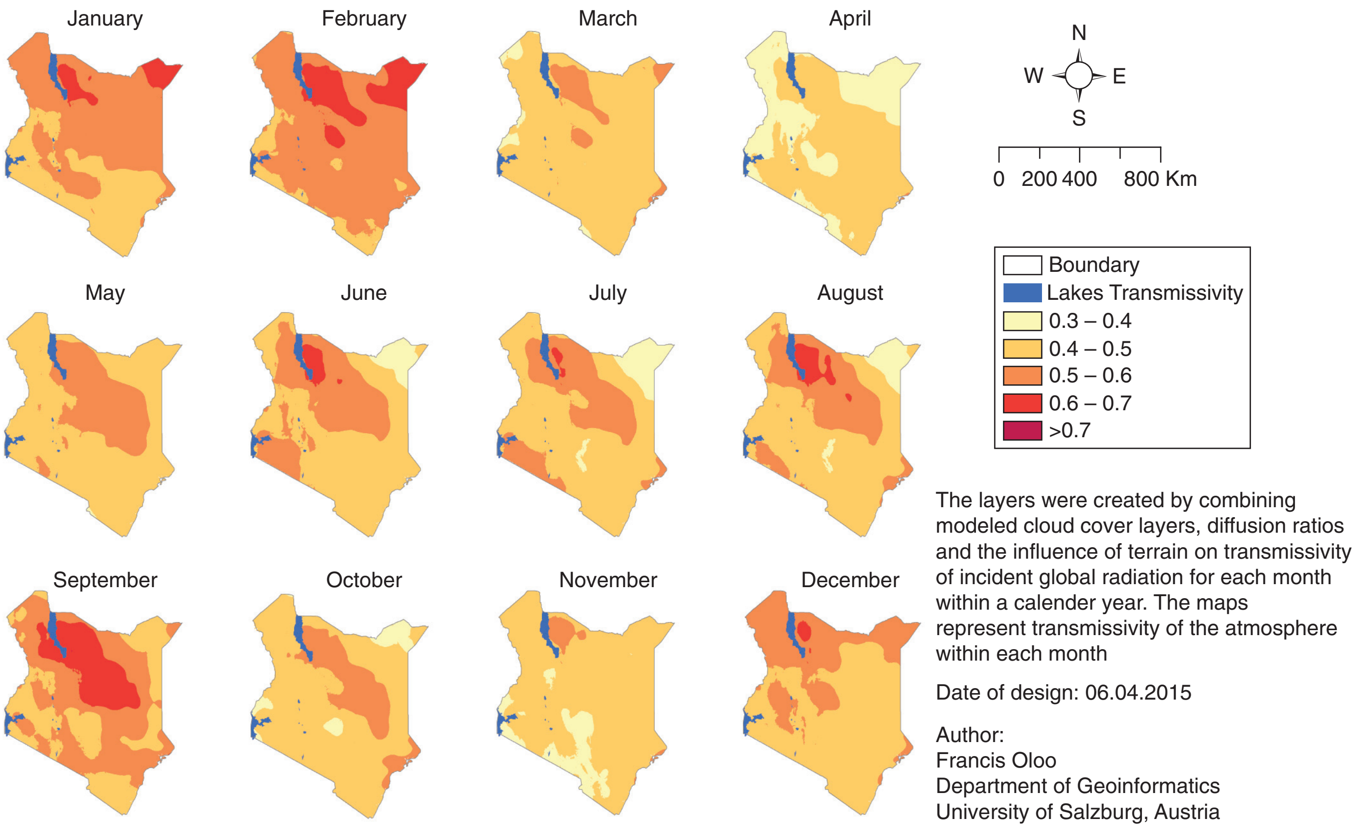

Figure 5: Estimated monthly transmissivity factors as modelled from cloud cover, diffuse ratio and elevation correction.

transmissivity factors at 7 TMY stations. The specific stations that were considered for comparison were Dagoreti, Garissa, Lodwar, Kisumu, Marsabit, Mombasa and Nyeri. The choice of these stations was mainly guided by their spatial distribution in different climatic regions in the country. A total of 84 data points (12 monthly data values in 7 stations) were used in the analysis. The root mean square error between the measured and the modelled transmissivity factors was 0.038 while the correlation coefficient between the measured and estimated factors was 0.84 indicating a positive correlation between the modelled transmissivity factors and the transmissivity factors which were calculated from measured meteorological variables at the TMY stations. Figure 6 shows the scatter plot of measured transmissivity factors against the estimated transmissivity factors.

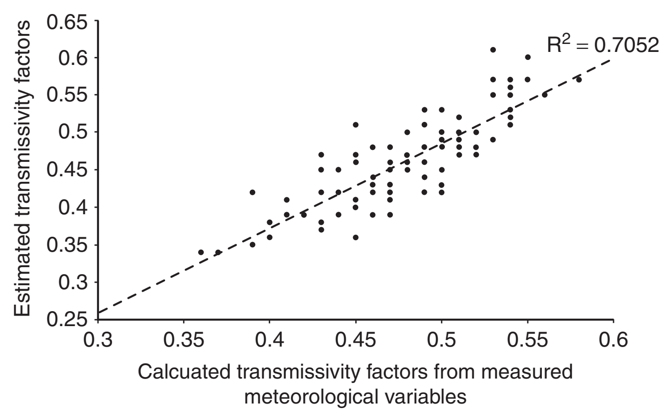

Figure 6: Scatter of plot of estimated transmissivity factors against calculated transmissivity factors.

3.3. Modelled monthly solar energy potential

Figure 7 represents maps of average daily solar energy potential for each month in Kenya. In each map the spatial distribution of solar energy potential in the area of study was mapped at 100 m spatial resolution.

From the maps of estimated monthly solar radiation, we observed that the months between March and September are generally characterised high values of solar radiation with large area of land in receiving radiation above 5 kWh/m^2/day. We particularly noted that in the month of May, the minimum value of estimated incident radiation was approximately 4.9 kWh/m^2/day

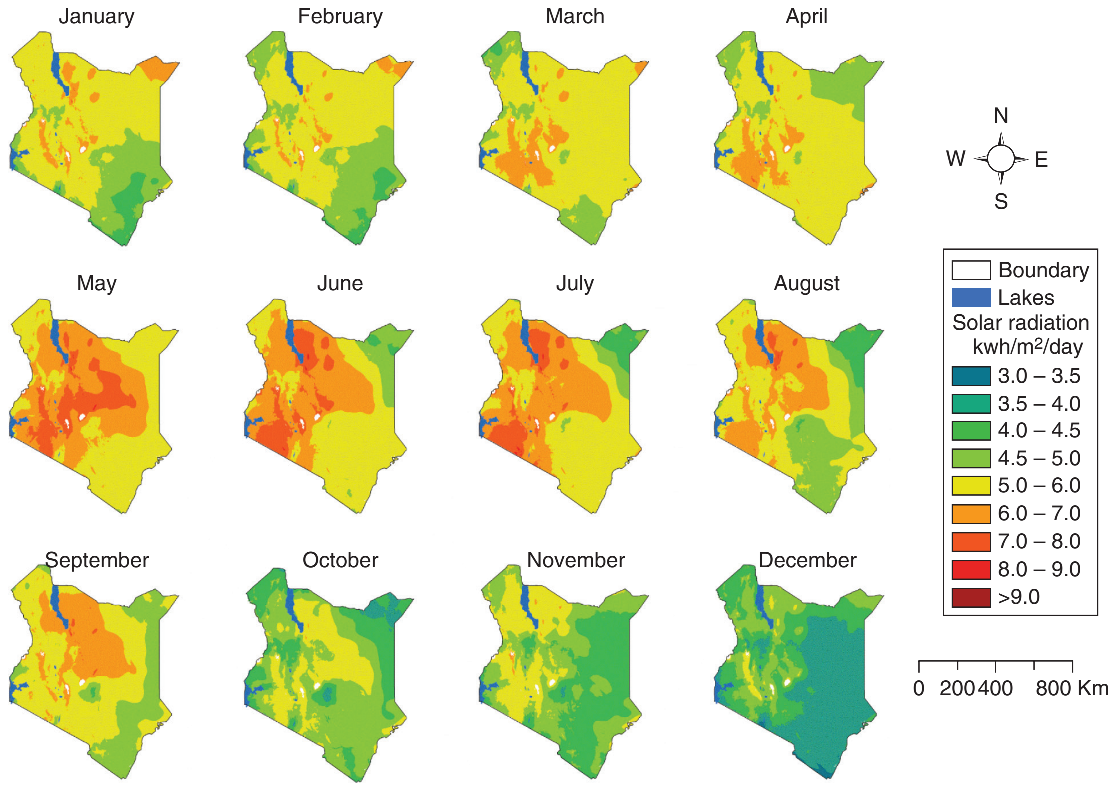

Figure 7: Estimated average daily solar energy potential (in kwh/m^2/day) for each month in Kenya.

while the average radiation in the same month was of 6.2 kWh/m^2/day. On the flipside however, the months of October, November and December recorded lower values of solar radiation with average estimated solar radiation of 4.72 kWh/m^2/day, 4.76 kWh/m^2/day and 4.14 kWh/m^2/day respectively. In the months between January and March, the average estimate solar radiation in the area of study was 5.4 kWh/m^2/day.

Figure 8 shows the box plot of estimated average daily radiation for each month in Kenya. The box indicates the interquartile range (25% and 75%); the line within the box represents the median and the bars represent the range of solar radiation potential in each month. The values are calculated from the pixel values of the estimated monthly solar radiation surfaces. The spatial resolution of each pixel was 100 by 100m. From the results, we observed that between March and September, the average solar energy potential in Kenya is generally above 5.5 kWh/m^2/day.

From the monthly solar radiation surfaces, we calculated an average annual solar radiation potential as shown in figure 3. From the maps, we observed that the highest values of annual solar radiation potential were observed in the regions neighbouring the rift valley and

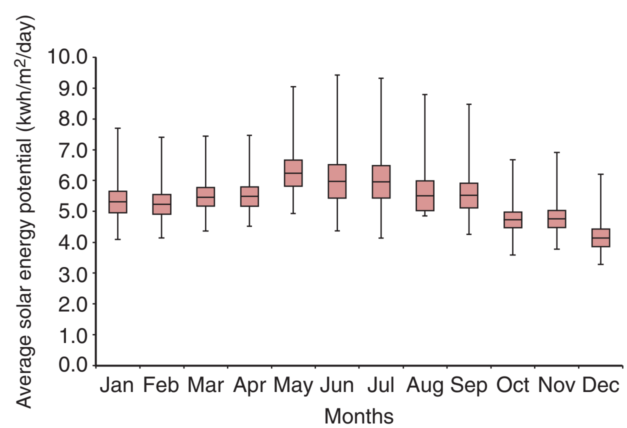

Figure 8: Estimated daily average solar energy potential for by month in Kenya.

also in the regions around Mt. Kenya. Similarly, high values of solar radiation potential were also recorded in the western region of Kenya, particular those that are near Mt. Elgon. Relatively lower potential areas were predicted in the costal planes and in the eastern regions of Kenya (mainly in the former North Eastern Province of Kenya).

Using the solar energy potential classes indicated in Figure 9b, we calculated the areas of land covered by the respective classes in Kenya. Figure 10 represents the

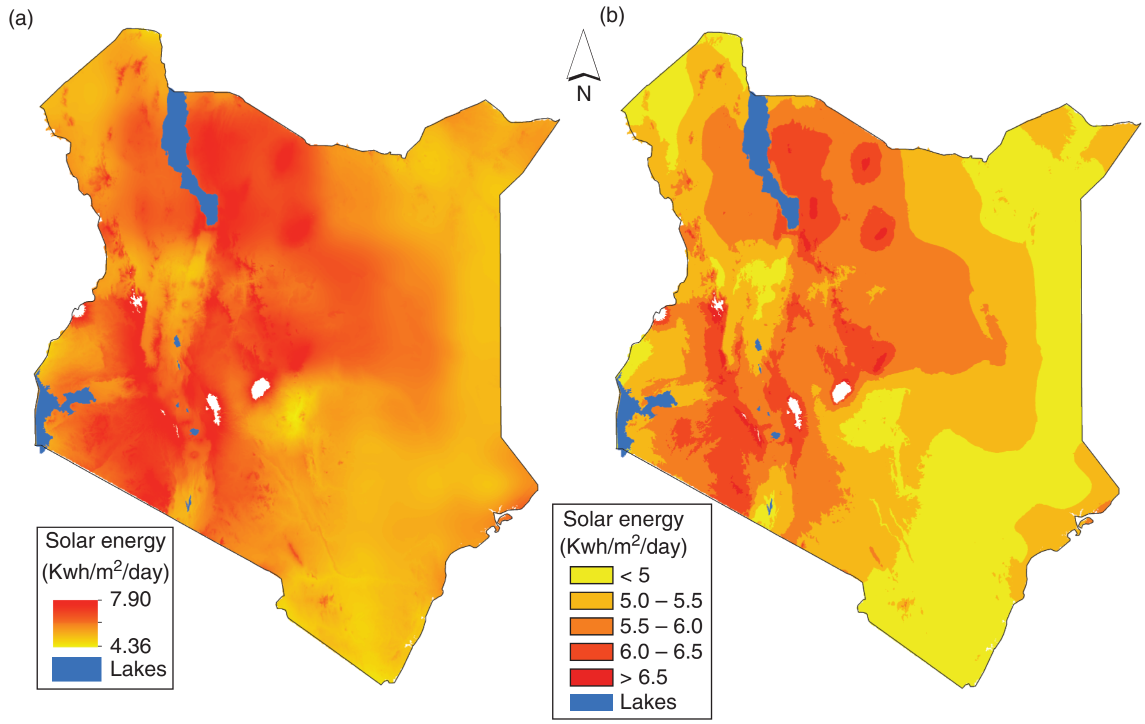

Figure 9: Spatial variation of solar energy potential in Kenya at 100 x 100m spatial resolution. a) Continuous average solar energy potential in kwh/m^2/day b) Classified average solar energy potential in kwh/m^2/day.

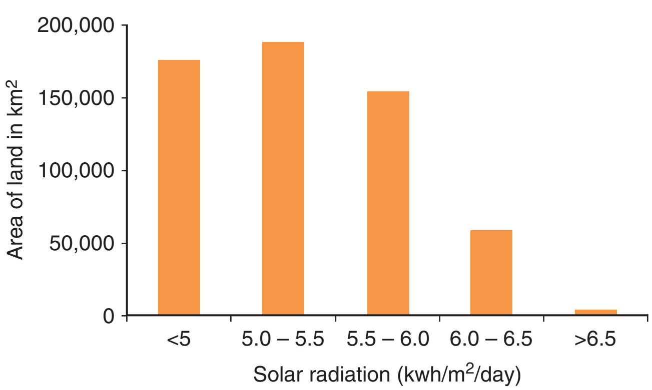

Figure 10: Areas of land characterized by different solar energy potential classes in Kenya.

areas of land in Kenya characterised by different classes of solar energy potential.

We noted that an area of approximately 188,284 km^2 (32.4%) of the total land the in Kenya was predicted to receive between 5.0-5.5 kWh/m^2/day of solar energy. Secondly, 154,185 km^2 (26.5%) of the land area was estimated to have a potential of receiving between 5.5-6.0 kWh/m^2/day. The third significant category was that which was estimated to receive between 6.0-6.5kWh/m^2/day of solar radiation, this occupied approximately 58,800 km^2(10.1%) of the land total land area. In the highest solar energy potential class, approximately 4,230 km^2 (0.7%) of the land area was characterised to receive more than 6.5 kWh/m^2/day of solar radiation. In the lowest solar energy potential category, approximately (176,170 km^2) 30.3% of the land area was estimated to receive less than 5 kWh/m^2/day of solar radiation.

3.4. Validation of modelled solar radiation estimates against the measured data

Measured monthly average solar radiation data from 7 TMY weather stations were compared with the modelled values at the stations from the monthly solar radiation surfaces. The selection of the 7 stations was based on the availability of long term measured climatic data and their spatial spread across the country. The stations whose data was used for validation were Dagoreti, Garissa, Lodwar, Kisumu, Marsabit, Mombasa and Nyeri. A total of monthly 84 data points (12 months in the seven stations) were used in the validation.

The mean error in the estimation of solar energy potential revealed low overall bias with a tendency to under-estimate radiation values by –0.29 kwh/m^2/day. The root mean square error was at 0.49. The correlation

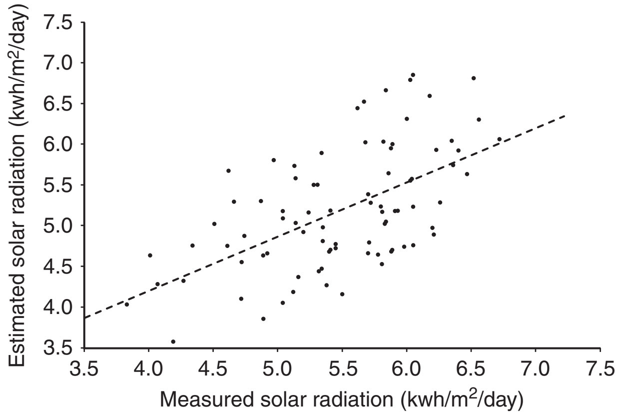

Figure 11: Scatter plot of measured versus estimated solar radiation for the validation set (n = 84).

between the measured and estimated values of solar radiation was 0.6 indicating a strong linear agreement as shown in Figure 5. The dotted line represents the line of best fit between the measured and the estimated values of solar radiation.

4. Conclusion

In this work, we successfully processed publicly available meteorological data and combined the same with estimated global radiation surfaces which were modelled within a GIS environment. The result was raster surface and statistics on the monthly and annual solar energy potential in Kenya. The plausibility of the main results from the study was confirmed by comparing the model results with measured data in cases where measured data was available.

From the study, we estimated that approximately 70% of the land area of Kenya has an annual solar energy potential above 5 kWh/m^2/day. Specifically 32.4% of the land has an average annual solar potential ranging between 5.0-5.5 kWh/m^2/day, additionally, approximately 26.5% of the country's land area has the average annual solar energy potential in the range of 5.5-6.0 kWh/m^2/day. Further still, above10.8% of the land area in Kenya has the potential of receiving more than 6 kWh/m^2/day of solar energy. The very high potential areas, that is, the areas which were estimated to receive solar radiation above 6 kWh/m^2/day were mainly located in the high altitude ridges of rift valley and also in the regions to the east of Lake Turkana and specifically around Marsabit. The spatial distribution of high potential areas in the country shows that investments in solar energy generation in the high potential areas can not only ensure adequate load for solar equipment but also increase the accessibility to electricity and other benefits of solar energy resources to more residents of the country especially those who inhabit far flung rural areas with little or no access to electricity at the moment.

In this study, we have been able to show that it possible to use publicly available data to accurately model solar irradiation at very high resolution, specifically we were able to model monthly solar radiation surfaces at 100m by 100m resolution in Kenya. We however note that integration of accurately measured meteorological data especially in mountainous areas into the solar energy models can greatly improve the accuracy of results. One of the challenges that we experienced in the course of this study was the general lack of up-to-date and long-term archives of measured meteorological data in the Kenya. We therefore recommended that in view, of the benefits that are likely to be accrued from the exploration and exploitation of renewable energy resources in Kenya specifically and in Africa in general, there is need to improve the network of meteorological stations and to make available the datasets from these stations to allow for research in natural resources and specifically renewable energy resources. The model that we implemented in this study mainly relied on the topographic characteristics of the area of study and on atmospheric transmissivity which we mainly estimated from cloud cover surfaces. We therefore recommended that broader models which allow for more covariates including precipitation, relative humidity and atmospheric aerosol content should be examined as a way of refining the results further. Finally, while the result from this study have been impressive, additional analysis on the economic viability of solar energy generation in the high potential areas should be carried out before any commercial projects are rolled out.

References

[1] Acker, R. & Kammen, D., (1996). The quiet (energy) revolution: analysing the dissemination of photovoltaic power systems in Kenya. In Energy Policy, 24(12). Available at: *https:// www.princeton.edu/pei/energy/publications/reports/No.287.pdf*

[2] Jaber, S.A. Al, (2012). Renewables 2012 Global Status report. REN21 Renewable Energy Policy Network/Worldwatch. Available at: *http://www.ren21.net/Portals/0/documents/Resources/GSR2012_low%20res_FINAL.pdf*

[3] Ondraczek, J. (2011). The Sun Rises in the East (of Africa): The Development and Status of the Solar Energy Markets in Kenya

and Tanzania. 2nd Symposium Small PV-Applications, Ulm, June. Available at: *http://www.fnu.zmaw.de/fileadmin/fnu-files/staff/ondraczek/110816_PVSEC_Paper_Janosch_Ondraczek_final.pdf*

[4] Kahle, A. B., Weill, G., Carter, W. D., Ulaby, F. T., Siqueira, P., Nashashibi, A., and Sarabandi, K. (2003). RADIATION (SOLAR). Proceedings of the IEEE, 63:137-147.

[5] Myers, D.(2003). Solar Radiation Modeling and Measurements for Renewable Energy Applications: Data and Model Quality; Preprint., (March). Available at: *http://www.osti.gov/energycitations/product.biblio.jsp?osti_id=15003726*

[6] Almorox, J., (2011). Estimating global solar radiation from common meteorological data in Aranjuez, Spain. In Turkish Journal of Physics,35: 53–64. Available at: *http://journals.tubitak.gov.tr/physics/issues/fiz-11-35-1/fiz-35-1-7-0912-20.pdf*

[7] Hena, M.A., Ali, M.S. and Rahman, M.M., (2013). A Simple Statistical Model to Estimate Incident Solar Radiation at the Surface from NOAA AVHRR Satellite Data. International Journal of Information Technology and Computer Science, 5(2): 36–41. Available at: *http://www.mecs-press.org/ijitcs/ijitcs-v5-n2/v5n2-4.html*

[8] Hammer, A., Heinemann, D., Hoyer, C., Kuhlemann, R., Lorenz, E., Müller, R., and Beyer, H. G. (2003). Solar energy assessment using remote sensing technologies. In Remote Sensing of Environment, 86(3): 423–432.

[9] Ramachandra, T. V, (2007). Solar energy potential assessment using GIS. In Energy Education & Technology, 18(2): 101–114.

[10] Ramachandra, T.V., Jain, R. and Krishnadas, G., (2011). Hotspots of solar potential in India. In Renewable and Sustainable Energy Reviews, 15(6): 3178–3186. Available at: *http://linkinghub.elsevier.com/retrieve/pii/S1364032111001444*

[11] Azhari, A. et al., (2008). A new approach for predicting solar radiation in tropical environment using satellite images-case study of Malaysia. WSEAS Transactions on Environment and Development, 4(4), pp.373–378. Available at: *http://www.wseas.us/e-library/transactions/environment/2008/30-870 N.pdf*

[12] Museruka, C. & Mutabazi, A., 2007. Assessment of Global Solar Radiation over Rwanda. International Conference on Clean Electrical Power 2007 (ICCEP'07), pp.670–676. *http://dx.doi.org/10.1109/ICCEP.2007.384312*

[13] Fadare, D. et al., (2010). Modeling of solar energy potential in Africa using an artificial neural network. American Journal of Scientific and Industrial Research, 1(2), pp.144–157. Available at: *http://www.scihub.org/AJSIR/PDF/2010/2/AJSIR-1-2-144-157.pdf*

[14] Rich, P. M., Dubayah, R., Hetrick, W. A., and Saving, S. C., (1994). Using viewshed models to calculate intercepted solar radiation: applications in ecology. American Society for Photogrammetry and Remote Sensing Technical Papers. In American Society of Photogrammetry and Remote Sensing: 524–529. Available at: *http://professorpaul. com/publications/rich_et_al_1994_asprs.pdf*

[15] Rich, Paul M., W.A.Hetrick and S.C.Saving, (1995). Modelling topographic influences on solar radiation. A manual for the SOLARFLUX model. Available at: *http://www.osti.gov/bridge/purl.cover.jsp?purl=/200698/*

[16] Quiquerez, L., Faessler, J., Lachal, B., Mermoud, F., & Hollmuler, P. GIS Methodology and case study regarding assessment of solar potential at territorial level: PV or thermal?. International Journal of Sustainable Energy Planning and Management (2015)

[17] Nguyen, H. T., & Pearce, J. M. (2010). Estimating potential photovoltaic yield with r. sun and the open source geographical resources analysis support system. Solar Energy, 84(5), 831–843.

[18] Ministry of Energy Kenya,.(2011). Scaling-Up Renewable Energy Program (SREP) .Draft SREP Investment Plan for Kenya. :1–66.

[19] Ministry of Energy Kenya, (2010). Feed-In-Tariffs Policy on Wind, Biomass , Small-Hydro , Geothermal , Biogas and Solar resource generated electricity: 1–15.

[20] Abdallah SM, Bressers H, Clancy JS. Energy Reforms in The Developing World: Sustainable Development Compromised? Int J Sustainable Energy Plan Manage 5 (2015) pages 41–56. *http://dx.doi.org/10.5278/ijsepm%20.2015.5.5*

[21] Hankins, M., Saini, A. & Karai, P. (2009). Target Market Analysis: Kenya's Solar Energy Market. Gesellschaft für technische Zusammenarbeit (GTZ) GmbH.

[22] Jacobson, A., (2007). Connective Power: Solar Electrification and Social Change in Kenya. World Development, 35(1):144–162. Available at: *http://linkinghub.elsevier.com/retrieve/pii/S0305750X06001860*

[23] Schillings C, Mayer R, Trieb F. (2004). High resolution solar radiation assessment forKenya: SWERA Report.

[24] Rabah KV. (2005). Integrated solar energy systems for rural electrification in Kenya. Renewable Energy, 30(1), 23–42.

[25] Kiplagat, J. K., Wang, R. Z., & Li, T. X. (2011). Renewable energy in Kenya: Resource potential and status of exploitation. Renewable and Sustainable Energy Reviews, 15(6), 2960–2973.

[26] Theuri, D., & Hamlin, T. (2008). Solar and wind energy resource assessment: Kenya country report. SWERA Project.

[27] OpenEI, (2013). SWERA/TMY Resource Information | Open Energy Information. Available at: *http://en.openei.org/wiki/SWERA/TMY_ Resource_Information*

[28] NASA, 2013. Surface meteorology and Solar Energy. A renewable energy resource website (Release 6.0) Available at: *http://eosweb.larc.nasa.gov/cgi-bin/sse/sse.cgi?oloofrank@gmail.com+s01#s01 [Accessed March 24, 2013].*

[29] Pons, X. and Ninyerola, M., (2008). Mapping a topographic global solar radiation model implemented in a GIS and refined with ground data. International Journal of Climatology, 28, pp.1821–1834. Available at *http://onlinelibrary.wiley.com/doi/10.1002/joc.1676/epdf*

[30] Dobrowski, S.Z., (2011). A climatic basis for microrefugia: the influence of terrain on climate. In Global Change Biology, 17(2): 1022–1035. Available at: *http://doi.wiley.com/10.1111/j.1365-2486.2010.02263.x*

[31] Bintanja, R., (1996). The parameterization of shortwave and longwave radiative fluxes for use in zonally averaged climate models. Journal of climate, 9(2): 439–454. Available at: *http://cat.inist.fr/?aModele=afficheN&cpsidt=3012977*

[32] Pellicciotti, F. et al., (2011). Transmission of solar radiation through clouds on melting glaciers: a comparison of parameterizations and their impact on melt modelling. Journal of Glaciology, 57(202), pp.367–381.

[33] Huang, S. *et al*., (2008). Modeling Monthly Near-Surface Air Temperature from Solar Radiation and Lapse Rate:Application over Complex Terrain in Yellowstone National Park. Physical Geography, 29(2), pp.158–178.

[34] Dubayah, R., and Rich, P., (1995). Topographic solar radiation models for GIS. International Journal of Geographical Information Systems. Available at: *http://www.tandfonline.com/doi/full/10.1080/02693799508902046*